MATCH
Communications in Mathematical and in Computer Chemistry

MATCH Commun. Math. Comput. Chem. **94** (2025) 195–214
ISSN: 0340–6253
doi: 10.46793/match.94-1.195C

Stability Analysis and Turing Pattern of An Enzyme-Catalyzed Reaction Model

Mengxin Chen[a] *, **Xue-Zhi Li**[a,b]

a. School of Mathematics and Statistics , Henan Normal University, Xinxiang 453007, P. R. China

b. School of Statistics and Mathematics, Henan Finance University, Zhengzhou 450046, P. R. China

chmxdc@163.com, xzli66@126.com

(Received October 15, 2024)

Abstract

This article reports the spatio-temporal dynamics of a diffusive enzyme-catalyzed system. When spatial diffusion is absent, we perform the stability analysis and explore the Hopf bifurcation of the system. We also determine the stability of the periodic solution resulting from the Hopf bifurcation. In what follows, for the diffusive enzyme-catalyzed system, the precise occurrence conditions of the Turing instability are given. Finally, some complex pattern phenomena of the system are observed. The main contributions of this paper are: (1) The types of positive equilibrium are classified by adjusting the range of control parameter. (2) The strict Turing instability domain is outlined, theoretically. (3) Some complex pattern phenomena of the enzyme-catalyzed reaction system are observed by utilizing the numerical approach.

1 Introduction

Turing pattern formation is one of the important investigation fields in the nonlinear reaction-diffusion systems owing to the pioneering work of

*Corresponding author.

Turing [1]. Chemical reaction systems are usually used to explore spatiotemporal pattern formation so that we can figure out the complex nonlinear dynamic of the systems [2–5]. Recently, much attention has been paid to exploring the complex spatiotemporal dynamic profiles of enzyme-catalyzed reactions. A typical enzyme-catalyzed reaction takes the form:

$$\begin{cases} \frac{du}{dt} = \alpha - F_1(u,v) - F_3(u), \\ \frac{dv}{dt} = \beta\left(F_1(u,v) - F_2(v)\right), \end{cases} \tag{1}$$

where u and v are the concentrations of the substrate S and product P, respectively, please refer to the reaction scheme diagram Fig. 1; $F_1(u,v)$ represents the rate law function of the substrate S and product P, which satisfies $F_1(0,v) = 0, \partial F_1/\partial u > 0$ and $\partial F_1/\partial v > 0$ for $u > 0$ and $v > 0$; moreover, $F_2(v)$ and $F_3(u)$ are sink rate functions of product P and substrate S, respectively; they are nonnegative, namely, $F_2(v) \geq 0$ and $F_3(u) \geq 0$ are valid in the enzyme-catalyzed reaction (1) for $u > 0$ and $v > 0$. The parameters α and β are positive kinetics constants. For more explanations with respect to this reaction scheme please refer to Refs. [6,7].

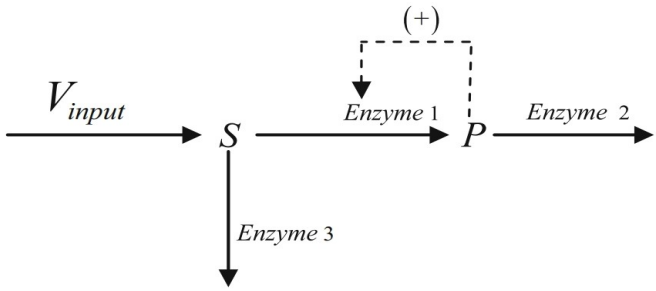

Figure 1. Reaction scheme diagram of the system (1) by involving three enzymes, where S is substrate and P describes the product. (This diagram can be also found in [6, 7].)

Let us recall some existing results with respect to (1). When $\beta = 1, F_1(u,v) = u^m v, F_2(v) = v/(v+1)$ and $F_3(u) = 0$, Leng et al. [8] reported the existence and nonexistence of periodic solutions by the aid of

Poincaré-Bendixson theorem and integral of divergence. When $F_1(u,v) = uv^m, F_2(v) = v/(v+1)$ and $F_3(u) = u$, Su [9] classified the types of the equilibria and discussed the existence of saddle-node bifurcation, Bogdanov-Takens bifurcation and Hopf bifurcation. A similar local bifurcation dynamic analysis of the enzyme-catalyzed reaction (1), such as the saddle-node, transcritical, pitchfork and Hopf bifurcations, has been also investigated by Zhang et al. [10] as $F_1(u,v) = uv, F_2(v) = v/(v+1)$ and $F_3(u) = u/(1+u)$. If $F_1(u,v) = uv, F_2(v) = v/(v+1)$ and $F_3(u) = u$ and consider the diffusion effect into the enzyme-catalyzed reaction (1), Atabaigi et al. [11] investigated the local stability of the constant steady state and they explored the occurrence conditions of the spatially homogeneous /nonhomogeneous periodic orbits and nonconstant steady states. For more existing dynamic results of system (1), please refer to [7, 12–15].

Owing to the diffusion process being a basic movement phenomenon in the real world, there are many nonlinear systems involving the diffusion effect, see Refs. [16–19]. Inspired by this aspect and suppose that $F_1(u,v) = uv^2, F_2(v) = v/(v+1)$ and $F_3(u) = 0$, one yields the following non-dimensional reaction diffusion version enzyme-catalyzed system:

$$\begin{cases} \frac{\partial u}{\partial t} = d_1 \Delta u + \alpha - uv^2, & \mathbf{x} \in \Omega, \quad t > 0, \\ \frac{\partial v}{\partial t} = d_2 \Delta v + \beta \left(uv^2 - \frac{v}{v+1} \right), & \mathbf{x} \in \Omega, \quad t > 0, \\ \frac{\partial u}{\partial \nu} = \frac{\partial v}{\partial \nu} = 0, & \mathbf{x} \in \partial\Omega, \quad t \geq 0, \\ u(\mathbf{x}, 0) = u_0(\mathbf{x}) \geq 0, \quad v(\mathbf{x}, 0) = v_0(\mathbf{x}) \geq 0, & \mathbf{x} \in \Omega, \end{cases} \tag{2}$$

where we assume that d_1 and d_2 represent the diffusion rates of the substrate u and product v at time t and location $\mathbf{x}$, respectively; Δ is the classical Laplacian operator; $\Omega \subset \mathbb{R}^N (N \geq 1)$ is a bounded region, ν is set to be the outward unit normal vector along the smooth boundary $\partial\Omega$. The condition $\frac{\partial u}{\partial \nu} = \frac{\partial v}{\partial \nu} = 0$ is the homogeneous Neumann boundary condition. Furthermore, we need to explain that the term $F_1(u,v) = uv^2$ is called cubic rate law and it can be found in other chemical reaction systems, see Refs. [7, 20, 21]. All parameters, d_1, d_2, α and β, are positive constants.

In this present paper, we shall perform the spatiotemporal dynamics of the enzyme-catalyzed reaction system (2). The reaction terms in the

enzyme-catalyzed reaction system (2) involve two parameters, namely, α and β. The case of the enzyme-catalyzed reaction system (1) with $\beta = 1$ has been studied in some existing literature (cf. [8]). However, in this paper, we can show that control parameter β plays a crucial role in analyzing and deducing the complex dynamics of the system (2) when $\beta \neq 1$. For the local system of (2), we give a stability and type classification of the constant steady state and the occurrence conditions of the Hopf bifurcation are also yielded by considering the range of β. For system (2), we perform the stability analysis of the constant steady state so that the emergence conditions of the Turing instability and Turing space can be presented when we choose β as the main critical parameter. In light of Turing instability, some complicated patterns are exhibited by choosing different values of β in Turing space.

This paper is structured as follows. In Sec. 2, the stability conditions of the positive equilibrium and the emergence conditions of the Hopf bifurcation are explored for the local system. In Sec. 3, one establishes the occurrence of the Turing instability for system (2). In Sec. 4, complex patterns of the system (2) are displayed with the aid of the numerical approach. We end this paper with some conclusions in Sec. 5.

2 Analysis of local temporal system

Without diffusion, the enzyme-catalyzed reaction system (2) has the form:

$$\begin{cases} \frac{du}{dt} = \alpha - uv^2, \\ \frac{dv}{dt} = \beta \left(uv^2 - \frac{v}{v+1} \right). \end{cases} \tag{3}$$

Define $f(u,v) = \alpha - uv^2$ and $g(u,v) = \beta \left(uv^2 - \frac{v}{v+1} \right)$. As such, it is easy to see that the model (3) enjoys a unique constant steady state, say E_*, where $E_* = \left(\frac{(1-\alpha)^2}{\alpha}, \frac{\alpha}{1-\alpha} \right)$ with the assumption $0 < \alpha < 1$. Now let us study the local asymptotically stability of this constant steady state E_*.

To achieve this goal, we can compute the Jacobian matrix at E_*:

$$J_0 = \begin{pmatrix} -\frac{\alpha^2}{(1-\alpha)^2} & 2(\alpha-1) \\ \frac{\beta\alpha^2}{(1-\alpha)^2} & \beta(1-\alpha^2) \end{pmatrix}.$$

In light of J_0, we can obtain the characteristic equation below:

$$\lambda^2 - T_0(\beta)\lambda + D_0(\beta) = 0, \tag{4}$$

where $T_0(\beta) = \beta(1-\alpha^2) - \frac{\alpha^2}{(1-\alpha)^2}$, $D_0(\beta) = \alpha^2\beta > 0$. To perform the types and stability of the constant steady state E_*, it is necessary to investigate the eigenvalues of the characteristic equation (4). To this end, we shall solve the eigenvalue λ, from (4), as follows:

$$\lambda_{1,2} = \frac{T_0(\beta) \pm \sqrt{T_0^2(\beta) - 4D_0(\beta)}}{2}.$$

Let

$$\beta_H = \frac{\alpha^2}{(1-\alpha^2)(1-\alpha)^2} > 0, \quad \beta^* = \frac{\alpha^2(3-\alpha) - 2\alpha^2\sqrt{2(1-\alpha)}}{(1-\alpha)(1-\alpha^2)^2} > 0 \tag{5}$$

and

$$\beta_* = \frac{\alpha^2(3-\alpha) + 2\alpha^2\sqrt{2(1-\alpha)}}{(1-\alpha)(1-\alpha^2)^2} > 0. \tag{6}$$

Now we can have the following.

Lemma 1. *Suppose that $0 < \alpha < 1$, then we claim that $\beta^* < \beta_H < \beta_*$.*

Proof. We can confirm the result is true by contradiction. Suppose that $\beta^* \geq \beta_H$. This is

$$\frac{\alpha^2(3-\alpha) - 2\alpha^2\sqrt{2(1-\alpha)}}{(1-\alpha)(1-\alpha^2)^2} \geq \frac{\alpha^2}{(1-\alpha^2)(1-\alpha)^2}.$$

This means that $3-\alpha-2\sqrt{2(1-\alpha)} \geq 1+\alpha$, namely, we can have $\alpha \leq -1$. This is impossible since we have restricted $0 < \alpha < 1$. Similarly, if we assume that $\beta_H \geq \beta_*$, then one must require that $\alpha - 1 \geq \sqrt{2(1-\alpha)}$.

Clearly, this case is incorrect since $0 < \alpha < 1$. Therefore, there holds $\beta^* < \beta_H < \beta_*$ for $0 < \alpha < 1$. We end the proof.

Theorem 1. *Suppose that $0 < \alpha < 1$ is valid, we build the following.*

(1) If $0 < \beta \leq \beta^*$, then the steady state E_* is a stable node;

(2) If $\beta^* < \beta < \beta_H$, then the steady state E_* is a stable focus;

(3) If $\beta_H < \beta < \beta_*$, then the steady state E_* is an unstable focus;

(4) If $\beta \geq \beta_*$, then the steady state E_* is an unstable node;

(5) If $\beta = \beta_H$, then the steady state E_* is a center.

Proof. To obtain our desired results, let $H(\beta) = T_0^2(\beta) - 4D_0(\beta)$. Then

$$H(\beta) = (1-\alpha^2)^2\beta^2 - \frac{2\alpha^2(3-\alpha)}{1-\alpha}\beta + \frac{\alpha^4}{(1-\alpha)^4}.$$

Let $H(\beta) = 0$, then it is easy to compute its root existence criterion, say $\Delta_{H(\beta)}$, is $\Delta_{H(\beta)} = \frac{32\alpha^4}{1-\alpha} > 0$ owing to $0 < \alpha < 1$. This implies that the equation $H(\beta) = 0$ must has two positive real solutions:

$$\beta^* = \frac{\alpha^2(3-\alpha) - 2\alpha^2\sqrt{2(1-\alpha)}}{(1-\alpha)(1-\alpha^2)^2},\ \beta_* = \frac{\alpha^2(3-\alpha) + 2\alpha^2\sqrt{2(1-\alpha)}}{(1-\alpha)(1-\alpha^2)^2}.$$

In view of β^* and β_*, one obtains $H(\beta) \geq 0$ if $0 < \beta \leq \beta^*$ or $\beta \geq \beta_*$. Moreover, $H(\beta) < 0$ if $\beta^* < \beta < \beta_*$ is valid.

(1) If $0 < \beta \leq \beta^*$ holds, by employing Lemma 1, we know that $0 < \beta \leq \beta^* < \beta_H$ must be satisfied. Accordingly, one gets $T_0(\beta) = \beta(1-\alpha^2) - \frac{\alpha^2}{(1-\alpha)^2} < \beta_H(1-\alpha^2) - \frac{\alpha^2}{(1-\alpha)^2} = 0$, i.e., $T_0(\beta) < 0$ for $0 < \beta \leq \beta^*$. On the other hand, it is noticed that $D_0(\beta) = \alpha^2\beta > 0$. So E_* is a stable node.

(2) If $\beta^* < \beta < \beta_H$ holds, then we have $H(\beta) < 0$ and $T_0(\beta) < 0$. Hence, all eigenvalues $\lambda_{1,2}$ of the characteristic equation (4) with negative real parts. It is suggested that the steady state E_* is a stable focus.

(3) If $\beta_H < \beta < \beta_*$ is satisfied, then we have $H(\beta) < 0$ and $T_0(\beta) = \beta(1-\alpha^2) - \frac{\alpha^2}{(1-\alpha)^2} > \beta_H(1-\alpha^2) - \frac{\alpha^2}{(1-\alpha)^2} = 0$. For this case, it is clear that all eigenvalues $\lambda_{1,2}$ of the characteristic equation (4) with positive real parts. As a result, the positive steady state E_* is an unstable focus.

(4) If $\beta \geq \beta_*$ is satisfied, this is $\beta > \beta_* > \beta_H$ by using Lemma 1. We immediately yield $T_0(\beta) > 0$ is fulfilled. Moreover, one has $H(\beta) > 0$ for

$\beta \geq \beta_*$. It is shown that all eigenvalues $\lambda_{1,2}$ of the characteristic equation (4) with positive real parts. Therefore, E_* is an unstable node.

(5) If $\beta = \beta_H$ holds, we can infer that $H(\beta) < 0$ since $\beta^* < \beta_H = \beta < \beta_*$ is valid. Also, it is easy to check that $T_0(\beta_H) = \beta_H(1-\alpha^2) - \frac{\alpha^2}{(1-\alpha)^2} = 0$. So the positive steady state E_* is a center. This ends the proof.

We have given a classification of the types and stability of the positive steady state E_*, please also see Fig. 2 to understand Theorem 1 better.

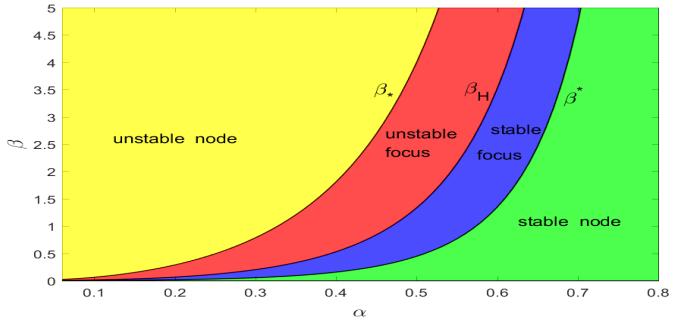

Figure 2. Stability and types of the unique positive constant steady state E_* in the plane of $\alpha - \beta$. In the "green domain", we can see that $0 < \beta \leq \beta^*$, so the constant steady state E_* is a stable node; in the "blue domain", we have $\beta^* < \beta < \beta_H$, thereby, the constant steady state E_* is a stable focus; in the "red domain", it is found that $\beta_H < \beta < \beta_*$, we claim that the constant steady state E_* is an unstable focus; finally, in the "yellow domain", clearly, one has $\beta \geq \beta_*$, so the constant steady state E_* is an unstable node.

Now let $\lambda = \chi(\beta) \pm i\delta(\beta)$ be the eigenvalue of (4), where

$$\chi(\beta) = \frac{\beta(1-\alpha^2)}{2} - \frac{\alpha^2}{2(1-\alpha)^2}, \quad \delta(\beta) = \frac{\sqrt{4D_0(\beta) - T_0^2(\beta)}}{2}.$$

Therefore, in light of (5) of Lemma 1, when $\beta = \beta_H$, then $\chi(\beta_H) = 0$ and $\delta(\beta_H) = \frac{\alpha^2}{1-\alpha}\sqrt{\frac{1}{1-\alpha^2}} > 0$. This shows that the characteristic equation (4) has a pair of purely imaginary roots. On the other hand, we can verify that $\chi'(\beta)|_{\beta=\beta_H} = \frac{1-\alpha^2}{2} > 0$. Therefore, the Poincaré Andronov-Hopf bifurcation theory indicates that enzyme-catalyzed model (3) surfers from the Hopf bifurcation at E_* as $\beta = \beta_H$.

The following result reports the direction of the Hopf bifurcation.

Theorem 2. *Suppose that* $0 < \alpha < 1$ *is valid. Then the enzyme-catalyzed reaction model* (3) *enjoys Hopf bifurcation when* $\beta = \beta_H = \frac{\alpha^2}{(1-\alpha^2)(1-\alpha)^2}$. *Furthermore, the Hopf bifurcation is supercritical (the periodic solution is stable) as* $\ell(\beta_H) < 0$, *however, the Hopf bifurcation is subcritical (the periodic solution is unstable) as* $\ell(\beta_H) > 0$, *where* $\ell(\beta_H)$ *can be found later.*

Proof. Making the transformations $\check{u} = u - \frac{(1-\alpha)^2}{\alpha}, \check{v} = v - \frac{\alpha}{1-\alpha}$ and still denoting $\check{u}, \check{v}$ by u, v, respectively. Then model (3) takes the form:

$$\begin{aligned}
\frac{du}{dt} =& m_{10}(\beta)u + m_{01}(\beta)v + m_{20}(\beta)u^2 + m_{11}(\beta)uv + m_{02}(\beta)v^2 \\
&+ m_{30}(\beta)u^3 + m_{21}(\beta)u^2v + m_{12}(\beta)uv^2 + m_{03}(\beta)v^3 + \mathcal{O}(|u,v|^4), \\
\frac{dv}{dt} =& n_{10}(\beta)u + n_{01}(\beta)v + n_{20}(\beta)u^2 + n_{11}(\beta)uv + n_{02}(\beta)v^2 \\
&+ n_{30}(\beta)u^3 + n_{21}(\beta)u^2v + n_{12}(\beta)uv^2 + n_{03}(\beta)v^3 + \mathcal{O}(|u,v|^4),
\end{aligned}$$

where $\mathcal{O}(|u,v|^4)$ are higher terms and

$$\begin{aligned}
&m_{10}(\beta) = -\frac{\alpha^2}{(1-\alpha)^2}, \quad m_{01}(\beta) = 2(\alpha-1), \quad m_{20}(\beta) = 0, \\
&m_{11}(\beta) = -\frac{2\alpha}{1-\alpha}, \quad m_{02}(\beta) = -\frac{(1-\alpha)^2}{\alpha}, \quad m_{12}(\beta) = -1, \\
&n_{10}(\beta) = \frac{\beta\alpha^2}{(1-\alpha)^2}, \quad n_{01}(\beta) = \beta(1-\alpha^2), \quad n_{20}(\beta) = 0, \quad n_{30}(\beta) = 0, \\
&n_{11}(\beta) = \frac{2\beta\alpha}{1-\alpha}, \quad n_{02}(\beta) = \beta(1-\alpha)^3 + \frac{\beta(1-\alpha)^2}{\alpha}, \quad n_{21}(\beta) = 0, \\
&n_{12}(\beta) = \beta, \quad n_{03}(\beta) = -\beta(1-\alpha)^4, \quad m_{30}(\beta) = m_{21}(\beta) = m_{03}(\beta) = 0.
\end{aligned}$$

To perform the direction of the Hopf bifurcation, we should determine the sign of the first Lyapunov number (see [22]). This is

$$\begin{aligned}
L_1(\beta) =& A\{[m_{10}(\beta)n_{10}(\beta)(m_{11}^2(\beta) + m_{11}(\beta)n_{02}(\beta) + m_{02}(\beta)n_{11}(\beta)) \\
&+ m_{10}(\beta)m_{01}(\beta)(n_{11}^2(\beta) + m_{20}(\beta)n_{11}(\beta) + m_{11}(\beta)n_{02}(\beta)) \\
&+ n_{10}^2(\beta)m_{02}(\beta)(m_{11}(\beta) + 2n_{02}(\beta)) - 2m_{10}(\beta)n_{10}(\beta)
\end{aligned}$$

$$
\begin{aligned}
&\times (n_{02}^2(\beta) - m_{20}(\beta)m_{02}(\beta)) - 2m_{10}(\beta)m_{01}(\beta)\\
&\times (m_{20}^2(\beta) - n_{20}(\beta)n_{02}(\beta)) - m_{01}^2(\beta)n_{20}(\beta)(2m_{20}(\beta) + n_{11}(\beta))\\
&+ (m_{01}(\beta)n_{10}(\beta) - 2m_{10}^2(\beta))(n_{11}(\beta)n_{02}(\beta) - m_{11}(\beta)m_{20}(\beta))]\\
&- (m_{10}^2(\beta) + m_{01}(\beta)n_{10}(\beta))[3(n_{10}(\beta)n_{03}(\beta) - m_{01}(\beta)m_{30}(\beta))\\
&+ 2m_{10}(\beta)(m_{21}(\beta) + n_{12}(\beta)) + (n_{10}(\beta)m_{12}(\beta) - m_{01}(\beta)n_{21}(\beta))]\}\\
=&A\ell(\beta),
\end{aligned}
$$

where $A = \frac{-3\pi}{2m_{01}(\beta)\mathrm{D}_0(\beta)^{3/2}}$ and

$$
\begin{aligned}
\ell(\beta) =& -\frac{2\alpha^4}{(1-\alpha)^4}\left(\frac{2\alpha^2}{(1-\alpha)^2} - \alpha\beta(1-\alpha)^2 - 2\beta(1-\alpha)\right)\\
&+ \frac{4\alpha^2}{1-\alpha}\left(\frac{2\beta\alpha^2}{(1-\alpha)^2} - \alpha(1-\alpha)^2 - (1-\alpha)\right)\\
&+ \frac{2\beta\alpha^2}{(1-\alpha)^3}\left(\alpha^2 - \alpha\beta(1-\alpha)^4 - \beta(1-\alpha)^3\right)\\
&+ 2\beta^2\alpha^4\left(1-\alpha+\frac{1}{\alpha}\right)^2 - 4\beta\left(\beta\alpha^2 + \frac{\alpha^4}{(1-\alpha)^3}\right)(\alpha(1-\alpha)+1)\\
&+ 3\left(\frac{\alpha^4}{(1-\alpha)^4} - \frac{2\beta\alpha^2}{1-\alpha}\right)\left(\beta\alpha^2(1-\alpha)^2 + \frac{\alpha^2}{(1-\alpha)^2}\right).
\end{aligned}
$$

Now at the Hopf bifurcation critical point $\beta_H = \frac{\alpha^2}{(1-\alpha^2)(1-\alpha)^2}$, one yields $D_0(\beta_H) = \frac{\alpha^4}{(1-\alpha^2)(1-\alpha)^2} > 0$ and $m_{01}(\beta_H) = 2(\alpha-1) < 0$, this is $A > 0$. Therefore, the first Lyapunov number $L_1(\beta_H)$ uniquely depends on the sign of $\ell(\beta_H)$, where we can not directly determine the sign of $\ell(\beta_H)$ since it is complex. However, one could still yield the desired results at the critical point $\beta = \beta_H$ by discussing the sign of $\ell(\beta_H)$. Precisely, the Hopf bifurcation is supercritical (the periodic solution is stable) as $\ell(\beta_H) < 0$, however, the Hopf bifurcation is subcritical (the periodic solution is unstable) as $\ell(\beta_H) > 0$. We finished the proof.

To verify the effectiveness of Theorem 2, we take $\alpha = 0.4$, then one obtains $E_* = (0.9000, 0.6667)$ and the Hopf bifurcation critical point is $\beta_H = 0.5291$. In this fashion, we obtain also $\ell(\beta_H) = -0.4571 < 0$. It is suggested that there are stable periodic solutions due to the supercritical

Hopf bifurcation, see Fig. 3.

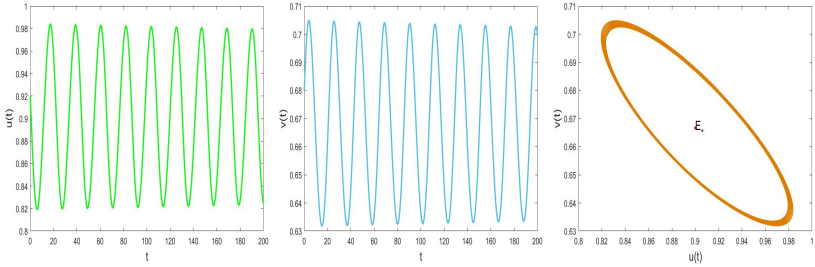

Figure 3. The enzyme-catalyzed reaction model (3) possesses the stable periodic solution due to the supercritical Hopf bifurcation, where one takes $\alpha = 0.4$ and $\beta = 0.5291$.

3 Turing instability

To yield the occurrence conditions of the Turing instability near E_*, let us first give the local linearized system of the enzyme-catalyzed model (2):

$$\frac{\partial}{\partial t}\begin{pmatrix} u \\ v \end{pmatrix} = L\begin{pmatrix} u \\ v \end{pmatrix} = D\begin{pmatrix} u \\ v \end{pmatrix} + J_0\begin{pmatrix} u \\ v \end{pmatrix}, \tag{7}$$

where

$$D = \begin{pmatrix} d_1\Delta & 0 \\ 0 & d_2\Delta \end{pmatrix}, \quad J_0 = \begin{pmatrix} -\frac{\alpha^2}{(1-\alpha)^2} & 2(\alpha-1) \\ \frac{\beta\alpha^2}{(1-\alpha)^2} & \beta(1-\alpha^2) \end{pmatrix}.$$

Considering the general solution of the local system (7), this is

$$\begin{pmatrix} u \\ v \end{pmatrix} = \begin{pmatrix} a_k \\ b_k \end{pmatrix} e^{\lambda_k t + i\mathbf{w}\cdot\mathbf{q}}, \tag{8}$$

where λ_k denotes by the characteristic spectrum for $k \in \mathbb{N}_0 = \{0, 1, 2, \cdots\}$, $\mathbf{w} = (k_x, k_y)$ is the wave number and there holds $k = |\mathbf{w}|$, $\mathbf{q} = (x, y)^T$ describes the spatial vector, i satisfies $i^2 = -1$, a_k and b_k are constants.

Putting (8) into (7), we can get

$$(J_k - \lambda_k I)\begin{pmatrix} a_k \\ b_k \end{pmatrix} e^{\lambda_k t + i\mathbf{w}\cdot\mathbf{q}} = 0,$$

where

$$J_k = \begin{pmatrix} -\frac{\alpha^2}{(1-\alpha)^2} - d_1 k^2 & 2(\alpha - 1) \\ \frac{\beta\alpha^2}{(1-\alpha)^2} & \beta(1-\alpha^2) - d_2 k^2 \end{pmatrix}.$$

Accordingly, we can get the following dispersion relation equation:

$$\lambda_k^2 - T_k(\beta)\lambda_k + D_k(\beta) = 0, \tag{9}$$

where

$$\begin{cases} T_k(\beta) = -(d_1 + d_2)k^2 + \beta(1-\alpha^2) - \frac{\alpha^2}{(1-\alpha)^2}, \\ D_k(\beta) = d_1 d_2 k^4 + \left[\frac{\alpha^2}{(1-\alpha)^2} d_2 - d_1\beta(1-\alpha^2)\right] k^2 + \beta\alpha^2. \end{cases}$$

In view of Turing's idea, we should first guarantee the positive constant steady state E_* is locally asymptotically stable for the enzyme-catalyzed reaction model (3), however, this positive constant steady state will lose its local stability as the diffusion effect is presented. This implies that we should further explore the stability problem of E_* for the reaction-diffusion enzyme-catalyzed model (2). Utilizing Theorem 1, it is find that for the local stability of E_*, we should only require that $0 < \beta < \beta_H$ is satisfied.

Now let us explore the stability result for E_* of the model (2).

Theorem 3. *Suppose that* $0 < \alpha < 1$ *and* $0 < \beta < \beta_H$ *are satisfied.*

(1) The positive constant steady state E_* *is locally asymptotically stable when* $\beta_1^* < \beta < \min\{\beta_H, \beta_2^*\}$*;*

(2) The positive constant steady state E_* *is unstable as* $\beta_H > \beta > \beta_2^*$ *or* $0 < \beta < \min\{\beta_H, \beta_1^*\}$*, where*

$$\beta_1^* = \frac{d_2\alpha^2(3-\alpha) - 2d_2\alpha^2\sqrt{2(1-\alpha)}}{d_1(1-\alpha)(1-\alpha^2)^2} = \beta^*\frac{d_2}{d_1} > 0, \tag{10}$$

and

$$\beta_2^* = \frac{d_2\alpha^2(3-\alpha) + 2d_2\alpha^2\sqrt{2(1-\alpha)}}{d_1(1-\alpha)(1-\alpha^2)^2} = \beta_* \frac{d_2}{d_1} > 0, \tag{11}$$

and β^* *and* β_* *have been defined in* (5) *and* (6).

Proof. Owing to $0 < \beta < \beta_H$ is satisfied, we immediately have $T_k(\beta) = -(d_1+d_2)k^2+\beta(1-\alpha^2)-\frac{\alpha^2}{(1-\alpha)^2} < -(d_1+d_2)k^2 < 0$ for all $k \in \mathbb{N}_0$. Hence, our following task is only exploring the sign of $D_k(\beta)$ since it will determine the stability of E_*. On the other hand, for the Turing instability, we should look for some conditions such that $D_k(\beta) < 0$ for some $k \in \mathbb{N}_0\backslash\{0\}$. This indicates that we have to ensure that

$$\beta > \frac{\alpha^2}{(1-\alpha^2)(1-\alpha)^2}\frac{d_2}{d_1} = \beta_H \frac{d_2}{d_1} > 0. \tag{12}$$

Now we are able to choose β as the critical parameter of the Turing instability. Considering the critical condition of the Turing instability, namely, $\min_{k_T \in \mathbb{N}_0\backslash\{0\}} D_{k_T}(\beta) = 0$, where $k_T \in \mathbb{N}_0\backslash\{0\}$ refers to the critical wave number of the Turing instability and it will be performed later. A straightforward calculation shows that $\min_{k_T \in \mathbb{N}_0\backslash\{0\}} D_{k_T}(\beta) := -\frac{\varphi(\beta)}{4d_1d_2} = 0$ with

$$\varphi(\beta) = d_1^2(1-\alpha^2)^2\beta^2 - \frac{2d_1d_2\alpha^2(3-\alpha)}{1-\alpha}\beta + \frac{d_2^2\alpha^4}{(1-\alpha)^4}.$$

Now we can obtain the potential critical values of the Turing instability by solving β from $\varphi(\beta) = 0$. They are:

$$\beta_1^* = \frac{d_2\alpha^2(3-\alpha) - 2d_2\alpha^2\sqrt{2(1-\alpha)}}{d_1(1-\alpha)(1-\alpha^2)^2} > 0,$$

and

$$\beta_2^* = \frac{d_2\alpha^2(3-\alpha) + 2d_2\alpha^2\sqrt{2(1-\alpha)}}{d_1(1-\alpha)(1-\alpha^2)^2} > 0.$$

Clearly, one obtains $\varphi(\beta) < 0$ when $\beta_1^* < \beta < \beta_2^*$ and $\varphi(\beta) > 0$ when $\beta > \beta_2^*$ or $0 < \beta < \beta_1^*$ is satisfied. Since we define $\min_{k_T \in \mathbb{N}_0\backslash\{0\}} D_{k_T}(\beta) := -\varphi(\beta) = 0$, one claims that $D_k(\beta) > 0$ when $\beta_1^* < \beta < \beta_2^*$ and $D_k(\beta) < 0$

when $\beta > \beta_2^*$ or $0 < \beta < \beta_1^*$ for some $k \in \mathbb{N}_0$. It is noticed that the assumption $0 < \beta < \beta_H$, then unique positive constant steady state E_* is locally asymptotically stable as $\beta_1^* < \beta < \min\{\beta_H, \beta_2^*\}$ and it becomes unstable as $\beta_H > \beta > \beta_2^*$ or $0 < \beta < \min\{\beta_H, \beta_1^*\}$. This ends the proof.

Benefiting from Theorem 3, we can establish the following result concerning the Turing instability.

Theorem 4. *Suppose that* $0 < \alpha < 1$ *and* $d_1 > d_2$ *are satisfied. Then the reaction-diffusion enzyme-catalyzed reaction mode* (2) *suffers from the Turing instability when* $\beta_T < \beta < \beta_H$ *with the critical wave number* $k = k_T$*, where* k_T *satisfies* $k^2 = k_T^2 = \sqrt{\frac{\beta_T \alpha^2}{d_1 d_2}}$ *and*

$$\beta_T = \frac{d_2\alpha^2(3-\alpha) + 2d_2\alpha^2\sqrt{2(1-\alpha)}}{d_1(1-\alpha)(1-\alpha^2)^2} > 0. \tag{13}$$

Proof. Theorem 3 tells us β_1^* or β_2^* may be the potential critical value of the Turing instability, see (10) and (11), respectively. Keeping this in mind and noting the necessary conditions for the Turing instability $0 < \beta < \beta_H$ and (12), i.e., $\beta > \beta_H \frac{d_2}{d_1}$, we immediately infer that the unique Turing instability critical value is $\beta = \beta_2^*$ since we have known that $\beta^* < \beta_H < \beta_*$ is valid, see Lemma 1. Therefore, the strictly Turing instability domain for the positive constant steady state E_* is $\beta_* \frac{d_2}{d_1} := \beta_T < \beta < \beta_H$. However, $\beta^* < \beta_H < \beta_*$ is true, so one must require that $d_2 < d_1$. Finally, recalling that $\min_{k_T \in \mathbb{N}_0 \setminus \{0\}} D_{k_T}(\beta) = 0$, we can obtain the critical wave number of the Turing instability is $k^2 = k_T^2 = \sqrt{\frac{\beta_T \alpha^2}{d_1 d_2}}$. This ends the proof.

4 Pattern formation: Numerical approach

In this subsection, we will perform the pattern formation of the reaction-diffusion enzyme-catalyzed reaction mode (2) in 2D computational domain $\Omega = (0, 50) \times (0, 50)$. According to the explicit Euler method, the reaction-diffusion enzyme-catalyzed reaction mode (2) can be discretized as follows:

$$\begin{cases} \frac{u_{ij}^{n+1} - u_{ij}^n}{\Delta t} = d_1 \Delta_d u_{ij}^n + \alpha - u_{ij}^n (v_{ij}^n)^2, \\ \frac{v_{ij}^{n+1} - v_{ij}^n}{\Delta t} = d_2 \Delta_d v_{ij}^n + \beta \left(u_{ij}^n (v_{ij}^n)^2 - \frac{v_{ij}^n}{1 + v_{ij}^n} \right), \end{cases} \tag{14}$$

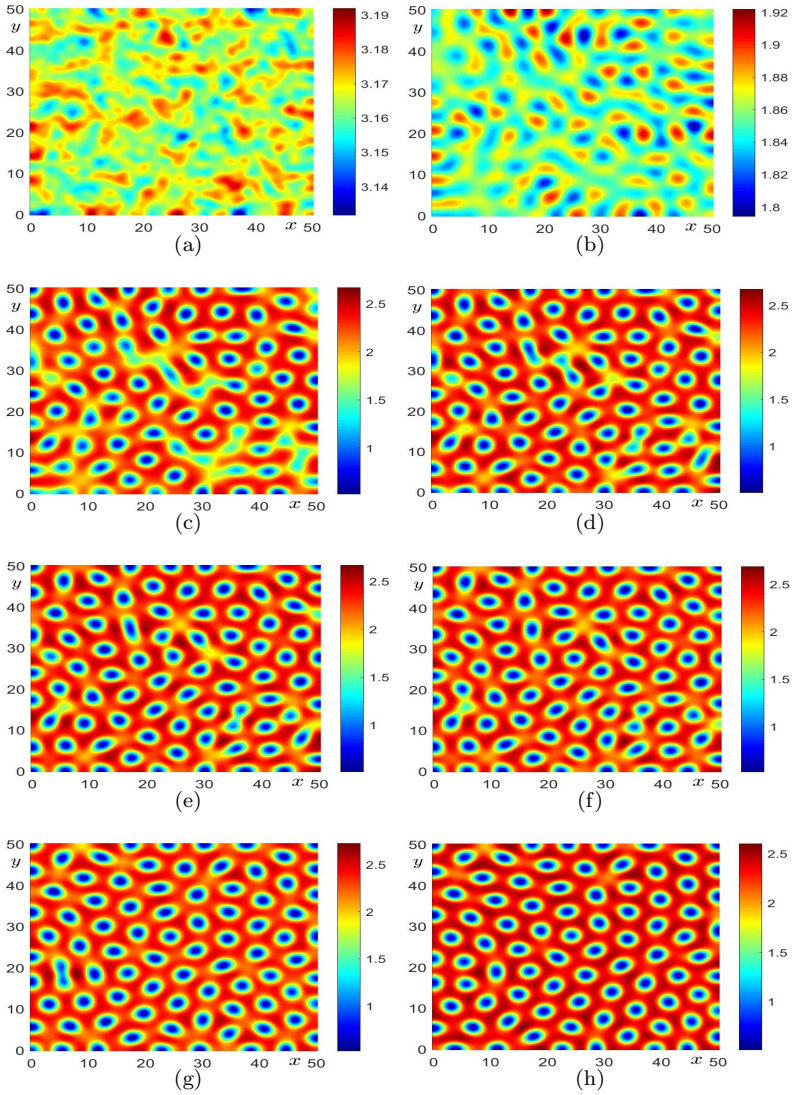

Figure 4. The enzyme-catalyzed reaction model (2) possesses the spot patterns when one takes $\alpha = 0.65, d_1 = 2.25, d_2 = 0.5$ and $\beta = 3.75$ with the initial data (15).

where

$$\Delta_d u_{ij}^n = \frac{u_{i+1,j}^n - 2u_{ij}^n + u_{i-1,j}^n}{\Delta x^2} + \frac{u_{i,j+1}^n - 2u_{ij}^n + u_{i,j-1}^n}{\Delta y^2}$$

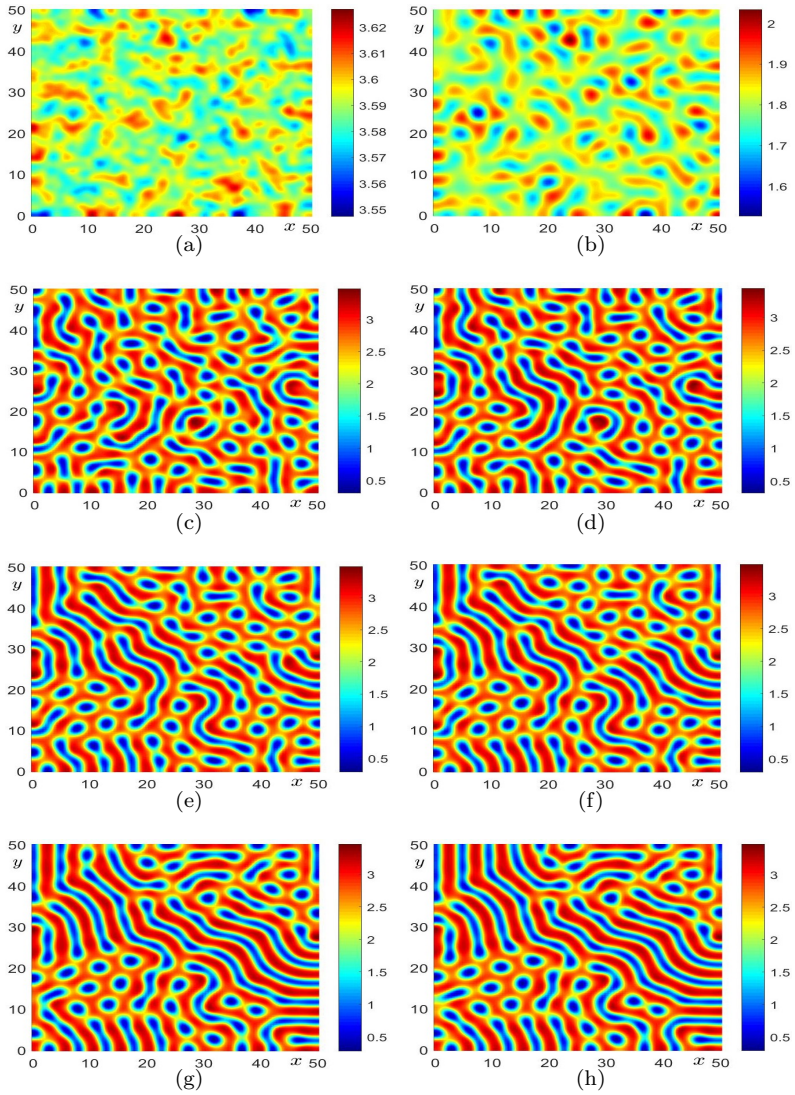

Figure 5. The enzyme-catalyzed reaction model (2) possesses the spot-stripe mixed patterns when choosing $\alpha = 0.65, d_1 = 2.25, d_2 = 0.5$ and $\beta = 5.15$ with the initial data (15).

and

$$\Delta_d v_{ij}^n = \frac{v_{i+1,j}^n - 2v_{ij}^n + v_{i-1,j}^n}{\Delta x^2} + \frac{v_{i,j+1}^n - 2v_{ij}^n + v_{i,j-1}^n}{\Delta y^2}.$$

where Δt is time step size and $n = 0, 1, \cdots$. By using the discrete Eq. (14), we can obtain the numerical approximate solution as follows:

$$\begin{cases} u_{ij}^{n+1} = u_{ij}^n + \Delta t[d_1 \Delta_d u_{ij}^n + \alpha - u_{ij}^n (v_{ij}^n)^2], \\ v_{ij}^{n+1} = v_{ij}^n + \Delta t \left[d_2 \Delta_d v_{ij}^n + \beta \left(u_{ij}^n (v_{ij}^n)^2 - \frac{v_{ij}^n}{1+v_{ij}^n} \right) \right]. \end{cases}$$

In our following content, we take the time step length $\Delta t = 0.01$ and the initial conditions are:

$$\begin{cases} u(x, y, 0) = u_* - 0.02 * \text{rand}(x, y), \\ v(x, y, 0) = v_* - 0.02 * \text{rand}(x, y), \end{cases} \tag{15}$$

where $\text{rand}(x, y)$ is a random variable between -1 and 1.

Firstly, we shall fix the parameters $\alpha = 0.65, d_1 = 2.25$ and $d_2 = 0.5$, then we obtain the positive constant steady state $E_* = (0.1885, 1.8571)$, the Hopf bifurcation threshold is $\beta_H = 5.9723$, and the Turing instability critical point is $\beta_T = 3.2361$. Therefore, with the help of Theorem 4, we know that the Turing instability domain is $3.2361 < \beta < 5.9723$.

(A) Taking $\beta = 3.75$ in the enzyme-catalyzed reaction model (2). The numerical result can be found in Fig. 4. Initially, there are no patterns formatting in the bounded domain Ω, see (a) of Fig. 4. However, with the increase of the reaction time t, a small number of irregular spots begin to appear in the fixed domain, see (b) of Fig. 4. These patterns become clearer with the competition of the substances u and v and they occupy the whole domain, see pictures (c)-(f) of Fig. 4. Finally, the shape of this spot pattern will not change with the random perturbation of the initial data (15), see the last two pictures (g)-(h) of Fig. 4.

(B) Now let us maintain $\beta = 5.15$, obviously, we have $3.2361 < \beta < 5.9723$. The numerical experiment result has been performed in Fig. 5. When the time t is short, there are no clear patterns that appear in the domain, see (a) and (b) of Fig. 5. However, this phenomenon is transient since the stripe and spot patterns rapidly occupy the bounded region with the random perturbation of the initial data (15), see pictures (c)-(f) of Fig. 5. In fact, they are mixed patterns. It is not difficult to observe that such a mixed pattern will not change its shape although the reaction time t is

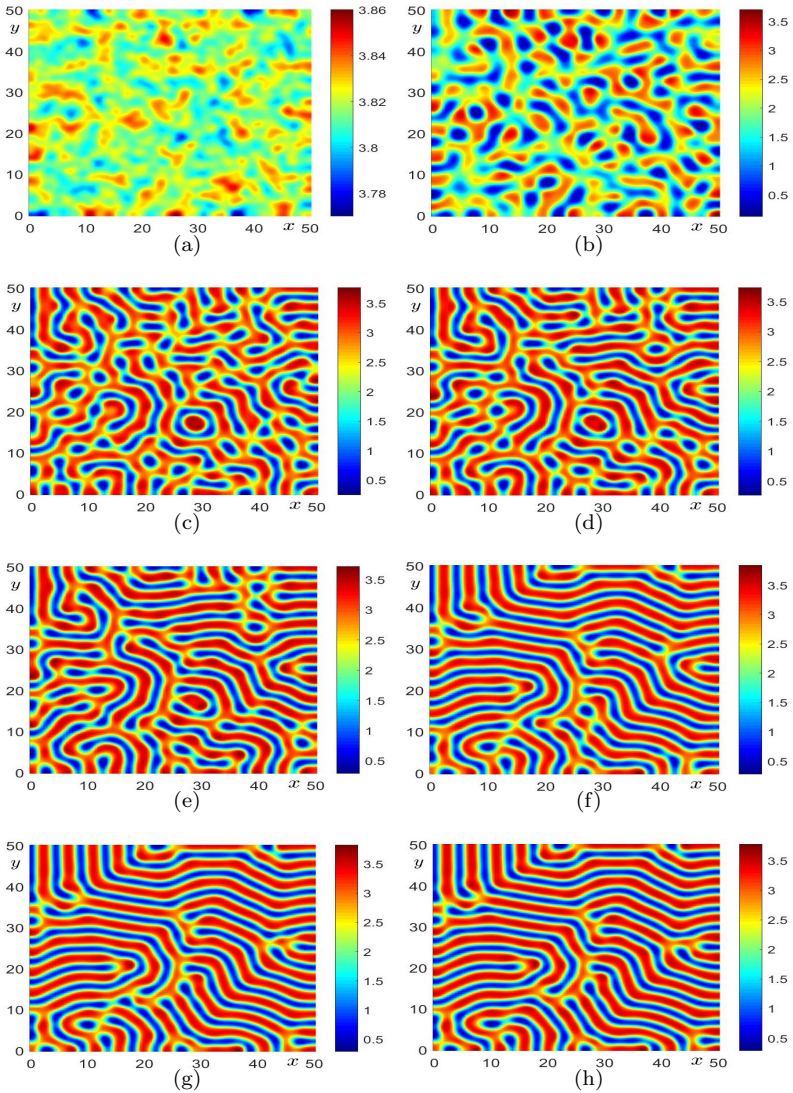

Figure 6. The enzyme-catalyzed reaction model (2) possesses the stripe patterns when we take $\alpha = 0.65, d_1 = 2.25, d_2 = 0.5$ and $\beta = 5.95$ with the initial data (15).

increasing, please refer to (g) and (h) of Fig. 5.

(C) In the Turing instability domain $3.2361 < \beta < 5.9723$, we choose

the control parameter $\beta = 5.95$. It is suggested that the enzyme-catalyzed reaction model (2) possesses the stripe patterns, see Fig. 6. Initially, there are some irregular mixed patterns filling the domain, see (a) and (b) of Fig. 6. This pattern phenomenon could be easily observed when we increase the reaction time t, refer to (c) and (d) of Fig. 6. However, as reaction time t increases, an interesting phenomenon is the spot patterns gradually disappear and the stripe patterns begin to capture the whole domain, see pictures (e) and (f) of Fig. 6. Finally, the pure stripe patterns occupy the domain and they do not change the shapes as the increase of reaction time t, please refer to the last two pictures (g) and (h) of Fig. 6.

5 Conclusions

In this paper, we study the temporal and spatial dynamics of a reaction diffusion enzyme-catalyzed reaction system with cubic rate law. For the non-diffusive system, the stable and unstable node and focus are classified by investigating the parameter range of β, see Theorem 1. In particular, if the equilibrium is a center, one shows that subcritical or supercritical Hopf bifurcation will occur for the non-diffusive system, see Theorem 2. In what follows, we turn our attention to the spatiotemporal system. When diffusion is integrated into the system, the positive equilibrium may change its local stability. In this manner, we obtain the conditions to ensure the existence of Turing instability, see Theorem 3 and Theorem 4, respectively. Finally, various complex spatial patterns are found in the enzyme-catalyzed reaction system (2), see Figs. 4-6, respectively. We hope that these results will help us to understand the interaction dynamics of the substrate and product for an enzyme-catalyzed reaction system.

***Acknowledgment*:** The authors express their sincere thanks to the anonymous reviewers for their comments on revisions. This work was supported by the National Natural Science Foundation of China (No. 12271143), the China Postdoctoral Science Foundation (No. 2021M7011-18), and Key Scientific Research Project of Henan Higher Education Institutions (No. 25A110008).

References

[1] A. M. Turing, The chemical basis of morphogenesis, *Phil. Trans. Roy. Soc. Lond. Ser. B* **237** (1999) 37–72.

[2] X. P. Yan, J. Y. Chen, C. H. Zhang, Dynamics analysis of a chemical reaction-diffusion model subject to Degn-Harrison reaction scheme, *Nonlin. Anal. Real World Appl.* **48** (2019) 161–181.

[3] R. C. Wu, L. L. Yang, Bogdanov-Takens bifurcation of codimension 3 in the Gierer-Meinhardt model, *Int. J. Bifurc. Chaos* **33** (2023) #2350163.

[4] L. Zhang, C. R. Tian, Turing pattern dynamics in an activator-inhibitor system with superdiffusion, *Phys. Rev. E* **90** (2014) #062915.

[5] B. Fercec, M. Dukarić, O. O. Aybard, I. K. Aybar, Supercritical Hopf bifurcations in two biochemical reaction systems, *MATCH Commun. Math. Comput. Chem.* **85** (2021) 525–544.

[6] J. Liu, Coordination restriction of enzyme-catalysed reaction systems as nonlinear dynamical systems, *Proc. Royal Soc. London A* **455** (1999) 285–298.

[7] J. Su, B. Xu, Local bifurcations of an enzyme-catalyzed reaction system with cubic rate law, *Nonlin. Dyn.* **94** (2018) 521–539.

[8] Z. Leng, B. Gao, Z. Wang, Qualitative analysis of a generalized system of saturated enzyme reactions, *Math. Comput. Model.* **49** (2009) 556–562.

[9] J. Su, Bifurcation analysis of an enzyme reaction system with general power of autocatalysis, *Int. J. Bifurc. Chaos* **29** (2019) #1950079.

[10] Q. Zhang, L. Liu, W. Zhang, Local bifurcations of the enzyme-catalyzed reaction comprising a branched network, *Int. J. Bifurc. Chaos* **25** (2015) #1550081.

[11] A. Atabaigi, A. Barati, H. Norouzi, Bifurcation analysis of an enzyme-catalyzed reaction-diffusion system, *Comput. Math. Appl.* **75** (2018) 4361–4377.

[12] W. Ko, Bifurcations and asymptotic behavior of positive steady-states of an enzyme-catalyzed reaction-diffusion system, *Nonlinearity* **29** (2016) 3777–3809.

[13] J. Su, Z. Wang, Global dynamics of an enzyme-catalyzed reaction system, *Bull. Malay. Math. Soc.* **43** (2020) 1919–1943.

[14] K. Kwek, W. Zhang, Periodic solutions and dynamics of a multimolecular reaction system, *Math. Comput. Model.* **36** (2002) 189–201.

[15] F. Davidson, R. Xu, J. Liu, Existence and uniqueness of limit cycles in an enzyme-catalysed reaction system, *Appl. Math. Comput.* **127** (2002) 165–179.

[16] M. X. Chen, S. Ham, J. Kim, Patterns of a general chemical model involving Degn-Harrison reaction scheme, *MATCH Commun. Math. Comput. Chem.* **93** (2025) 267–290.

[17] H. Sha, L. Zhu, Dynamic analysis of pattern and optimal control research of rumor propagation model on different networks, *Inf. Process. Manag.* **62** (2025) #104016.

[18] R. Han, L. N. Guin, B. Dai, Consequences of refuge and diffusion in a spatiotemporal predator-prey model, *Nonlin. Anal. Real World Appl.* **60** (2021) #103311.

[19] M. X. Chen, R. C. Wu, Dynamics of a harvested predator-prey model with predator-taxis, *Bull. Malay. Math. Sci. Soc.* **46** (2023) #76.

[20] P. Tracqui, A. Perault-Staub, G. Milhaud, J. F. Staub , Theoretical study of a two-dimensional autocatalytic model for calcium dynamics at the extracellular fluid-bone interface, *Bull. Math. Biol.* **49** (1987) 597–613.

[21] P. Gray, S. Scott, Autocatalytic reactions in the isothermal, continuous stirred tank reactor. Isolas and other forms of multistability, *Chem. Eng. Sci.* **38** (1983) 29–43.

[22] L. Perko, *Differential Equations and Dynamical Systems*, Springer, New York, 2001.